Positive and negative parity hyperons in nuclear medium

K. Azizi[1] *, N. Er[1,2]†, H. Sundu[3]‡

[1] Department of Physics, Doğuş University, Acıbadem-Kadıköy, 34722 İstanbul, Turkey

[2] Department of Physics, Abant İzzet Baysal University, Gölköy Kampüsü, 14980 Bolu, Turkey

[3] Department of Physics, Kocaeli University, 41380 İzmit, Turkey

Abstract

The effects of nuclear medium on the residue, mass and self energy of the positive and negative parity Σ, Λ and Ξ hyperons are investigated using the QCD sum rule method. In the calculations, the general interpolating currents of hyperons with an arbitrary mixing parameter are used. We compare the results obtained in medium with those of the vacuum and calculate the shifts in the corresponding parameters. It is found that the shifts on the residues in nuclear matter are over all positive for both the positive and negative parity hyperons, except for the positive parity Σ hyperon that the shift is negative. The shifts on the masses of these baryons are obtained to be negative. The shifts on the residues and masses of negative parity states are large compared to those of positive parities. The maximum shift belongs to the residue of the negative parity Λ hyperon. The vector self-energies gained by the positive parity baryons are large compared to the negative parities' vector self-energies. The maximum value of the vector self-energy belongs to the positive parity Σ hyperon. The numerical values are compared with the existing predictions in the literature.

PACS number(s): 14.20.Jn, 21.65.-f, 11.55.Hx

*e-mail: kazizi@dogus.edu.tr
†e-mail: nuray@ibu.edu.tr
‡e-mail: hayriye.sundu@kocaeli.edu.tr

1 Introduction

The study of in medium properties of hadrons constitutes one of the main research directions in QCD. It helps us gain valuable knowledge on the structure of dense astrophysical objects like neutron stars, QCD phase diagram, as well as perturbative and non-perturbative natures of QCD. The investigation of in-medium hadronic parameters can also help us in analyzing the results of heavy ion collision experiments. The effects of nuclear medium on nucleon parameters have been widely investigated in the literature [1–5]. But, there are a few number of works dedicated to the study of these effects on the properties of strange members of the octet baryons. It is well known that the nucleons are affected by the nuclear medium considerably [5]. As Σ, Λ and Ξ hyperons have also u and d quarks content their inside, it is expected that their parameters are also affected by the medium. The investigation of hyperons in nuclear medium and the comparison of the results with the nucleons can helps us to determine the order of $SU(3)_f$ violation in medium. The predictions of the scalar and vector self-energies of these particles can also provide valuable information on the scalar and vector in-medium couplings of these particles. In [6], the authors study the self-energies of the Λ hyperon in nuclear medium using the finite-density QCD sum rules. Their calculations show that the vector and scalar self-energies of the Λ hyperon are substantially smaller than the corresponding nucleon self-energies. In [7], the authors apply the same method to investigate the self-energies of the Σ hyperon propagating in nuclear matter. They find that the Lorentz vector self-energy of Σ is similar to that of the nucleon. They show that the magnitude of Lorentz scalar self-energy of the Σ hyperon is close to the corresponding value of the nucleon; although it is sensitive to the strangeness content of the nucleon and to the density dependence of certain four-quark condensate. In [8], the authors consider mass shifts for the baryon octet using a model independent approach to baryon-baryon interactions based on the chiral perturbation theory. In [9], the authors have applied the chiral quark-meson coupling (CQMC) model by including the effects of gluon and pion exchanges to study the properties of hyperons in a nuclear matter. In [10], S. R. Beane et al. use $n\Sigma^-$ scattering phase shifts to quantify the energy shift of the Σ^- hyperon in dense neutron matter.

In the present work, we extend the above mentioned studies by including the negative parity hyperons. In particular, we use the QCD sum rule approach to calculate the shifts on the residues, masses and the self energies of Σ, Λ and Ξ hyperons due to the nuclear medium for both positive and negative parities. We use the most general form of the interpolating currents of these baryons and try to find reliable region for the general parameter entering

the interpolating fields. We compare the results obtained with existing predictions in the literature for the positive parity hyperons.

The article is organized as follow. In section 2, we obtain QCD sum rules for the residues, masses and self energies of the Σ, Λ and Ξ hyperons in the nuclear matter. Section 3 is devoted to the numerical analyses of the sum rules and the comparison of the results with the existing predictions as well as with the vacuum results. Section 4 contains our concluding remarks.

2 In-medium QCD sum rules for the residues, masses and self energies of hyperons

To obtain the QCD sum rules for the residues , masses and self energies of Σ, Λ, Ξ hyperons in the presence of nuclear matter, the starting point is to consider the following two-point correlation function:

$$\Pi(p) = i \int d^4x e^{ip\cdot x} \langle \psi_0 | T[J_H(x) \bar{J}_H(0)] | \psi_0 \rangle, \tag{2.1}$$

where p is the four momentum of the hyperon, $|\psi_0\rangle$ is the nuclear matter ground state and the subindex H is used for the Σ, Λ, Ξ hyperons. Here J_H is the related interpolating current coupling to both the positive and negative parities. The general form of J_H for the corresponding baryons are taken as [11, 12]

$$\begin{aligned}
J_\Sigma(x) &= -\frac{1}{\sqrt{2}}\epsilon_{abc}\sum_{i=1}^{2}\Big[\Big(u^{T,a}(x)CA_1^i s^b(x)\Big)A_2^i d^c(x) - \Big(d^{T,c}(x)CA_1^i s^b(x)\Big)A_2^i u^a(x)\Big], \\
J_\Lambda(x) &= \frac{1}{\sqrt{6}}\epsilon_{abc}\sum_{i=1}^{2}\Big[2\Big(u^{T,a}(x)CA_1^i d^b(x)\Big)A_2^i s^c(x) + \Big(u^{T,a}(x)CA_1^i s^b(x)\Big)A_2^i d^c(x) \\
&\quad + \Big(d^{T,c}(x)CA_1^i s^b(x)\Big)A_2^i u^a(x)\Big], \\
J_\Xi(x) &= -\epsilon_{abc}\sum_{i=1}^{2}\Big(s^{T,a}(x)CA_1^i u^b(x)\Big)A_2^i s^c(x),
\end{aligned} \tag{2.2}$$

where a, b, c are color indices, C is the charge conjugation operator and $A_1^1 = I$, $A_1^2 = A_2^1 = \gamma_5$, $A_2^2 = \beta$. As previously said, the parameter β is an arbitrary auxiliary parameter, and $\beta = -1$ corresponds to the Ioffe current [13–16]. Considering the Lorentz covariance and parity invariance the correlation function can be decomposed as

$$\Pi(p) = \Pi_p \not{p} + \Pi_u \not{u} + \Pi_S I + \Pi'(p_\mu u_\nu - p_\nu u_\mu)\sigma^{\mu\nu}, \tag{2.3}$$

where the Π_i's and Π' are the functions of the invariants p^2 and $p\cdot u$ with u being the four vector velocity of the nuclear medium. In the calculations, we will use the structures $\not{p}, \not{u}$ and unit matrix I to construct the sum rules for the quantities under consideration. According to the method used, we calculate the aforesaid correlation function in two hadronic and OPE sides. Matching these two sides through a dispersion relation leads to the sum rules for the considered parameters.

2.1 Hadronic representation

The correlation function can be calculated by inserting complete sets of hyperon states with both parities and with the same quantum numbers as the interpolating currents. After performing integral over four-x, we get

$$\begin{aligned}\Pi^{Had} = &- \frac{\langle\psi_0|J_{H^+}(x)|H^+(p^*,s)\rangle\langle H^+(p^*,s)|\bar{J}_{H^+}(0)|\psi_0\rangle}{p^{*2}-m^{*2}_{H^+}} \\ &- \frac{\langle\psi_0|J_{H^-}(x)|H^-(p^*,s)\rangle\langle H^-(p^*,s)|\bar{J}_{H^-}(0)|\psi_0\rangle}{p^{*2}-m^{*2}_{H^-}} + ..., \end{aligned} \tag{2.4}$$

where $|H^+(p^*,s)\rangle$ and $|H^-(p^*,s)\rangle$ are the hyperon states with positive and negative parity, respectively and the dots represents the contributions of the higher states and the continuum. Here p^* is the four momentum and m^*_H is the mass of the hyperon in medium. The matrix elements appearing in Eq. (2.4) can be parametrized as

$$\begin{aligned}\langle\psi_0|J_{H^+}(x)|H^+(p^*,s)\rangle &= \lambda^*_{H^+}u_{H^+}(p^*,s), \\ \langle\psi_0|J_{H^-}(x)|H^-(p^*,s)\rangle &= \lambda^*_{H^-}\gamma_5 u_{H^-}(p^*,s), \end{aligned} \tag{2.5}$$

where $\lambda^*_{H^+}$ and $\lambda^*_{H^-}$ are the modified residues or the coupling strengths of the positive and negative parity hyperons, respectively; $u_{H^+}(p^*,s)$ and $u_{H^-}(p^*,s)$ are their Dirac spinors. Using Eq. (2.5) in Eq. (2.4) and summing over the spins of positive and negative parity hyperons, we get

$$\Pi^{Had} = -\frac{\lambda^{*2}_{H^+}(\not{p}^*+m^*_{H^+})}{p^{*2}-m^{*2}_{H^+}} - \frac{\lambda^{*2}_{H^-}(\not{p}^*-m^*_{H^-})}{p^{*2}-m^{*2}_{H^-}} + ..., \tag{2.6}$$

which can be written as

$$\begin{aligned}\Pi^{Had} &= -\frac{\lambda^{*2}_{H^+}}{\not{p}^*-m^*_{H^+}} - \frac{\lambda^{*2}_{H^-}}{\not{p}^*+m^*_{H^-}} + ... \\ &= -\frac{\lambda^{*2}_{H^+}}{(p^\mu_{H^+}-\Sigma^\mu_{\nu H^+})\gamma_\mu - (m_{H^+}+\Sigma^S_{H^+})} - \frac{\lambda^{*2}_{H^-}}{(p^\mu_{H^-}-\Sigma^\mu_{\nu H^-})\gamma_\mu + (m_{H^-}+\Sigma^S_{H^-})} + ... \end{aligned} \tag{2.7}$$

where $\Sigma^{\mu}_{\nu H^{\pm}}$ and $\Sigma^{S}_{H^{\pm}}$ are the vector and the scalar self-energies of the positive and negative parity hyperons in nuclear matter, respectively [17]. In general, we can write

$$\Sigma^{\mu}_{\nu H^{\pm}} = \Sigma_{\nu H^{\pm}} u^{\mu} + \Sigma'_{\nu H^{\pm}} p^{\mu}_{H^{\pm}}, \tag{2.8}$$

where $\Sigma_{\nu H^{\pm}}$ and $\Sigma'_{\nu H^{\pm}}$ are constants and u^{μ} is the four velocity of the nuclear medium. Here, we neglect $\Sigma'_{\nu H^{\pm}}$ due to its small contribution (see also [17]). Apart from the vacuum QCD calculations, the four-velocity of the nuclear matter is new concept that causes extra structures to the correlation function. We shall work in the rest frame of the hyperon with $u^{\mu} = (1, 0)$. Substitution of Eq. (2.8) into Eq. (2.7), the hadronic side of the correlation function can be written in terms of three different structure as

$$\Pi^{Had} = \Pi^{Had}_{p}(p^2, p_0) \not{p} + \Pi^{Had}_{u}(p^2, p_0) \not{u} + \Pi^{Had}_{S}(p^2, p_0) I + ..., \tag{2.9}$$

where p_0 is the energy of the quasi-particle and

$$\begin{aligned}
\Pi^{Had}_{p}(p^2, p_0) &= -\lambda^{*2}_{H^+} \frac{1}{p^2 - \mu^2_{H^+}} - \lambda^{*2}_{H^-} \frac{1}{p^2 - \mu^2_{H^-}}, \\
\Pi^{Had}_{u}(p^2, p_0) &= +\lambda^{*2}_{H^+} \frac{\Sigma_{H^+\nu}}{p^2 - \mu^2_{H^+}} + \lambda^{*2}_{H^-} \frac{\Sigma_{H^-\nu}}{p^2 - \mu^2_{H^-}}, \\
\Pi^{Had}_{S}(p^2, p_0) &= -\lambda^{*2}_{H^+} \frac{m^{*}_{H^+}}{p^2 - \mu^2_{H^+}} + \lambda^{*2}_{H^-} \frac{m^{*}_{H^-}}{p^2 - \mu^2_{H^-}}.
\end{aligned} \tag{2.10}$$

Here $m^{*}_{H^{\pm}} = m_{H^{\pm}} + \Sigma^{S}_{H^{\pm}}$ and $\mu^2_{H^{\pm}} = m^{*2}_{H^{\pm}} - \Sigma^2_{\nu H^{\pm}} + 2p_0^{H^{\pm}} \Sigma_{\nu H^{\pm}}$. After a Wick rotation and applying the Borel transformation with respect to p^2, we get

$$\begin{aligned}
\hat{B}\Pi^{Had}_{p}(p^2, p_0) &= \lambda^{*2}_{H^+} e^{-\mu^2_{H^+}/M^2} + \lambda^{*2}_{H^-} e^{-\mu^2_{H^-}/M^2}, \\
\hat{B}\Pi^{Had}_{u}(p^2, p_0) &= -\lambda^{*2}_{H^+} \Sigma_{\nu H^+} e^{-\mu^2_{H^+}/M^2} - \lambda^{*2}_{H^-} \Sigma_{\nu H^-} e^{-\mu^2_{H^-}/M^2}, \\
\hat{B}\Pi^{Had}_{S}(p^2, p_0) &= \lambda^{*2}_{H^+} m^{*}_{H^+} e^{-\mu^2_{H^+}/M^2} - \lambda^{*2}_{H^-} m^{*}_{H^-} e^{-\mu^2_{H^-}/M^2},
\end{aligned} \tag{2.11}$$

where M^2 is the Borel mass parameter.

2.2 OPE side

The OPE side of the correlation function can be calculated in deep Euclidean region. It can also be written in terms of the considered structures as

$$\Pi^{OPE}(p) = \Pi^{OPE}_{p} \not{p} + \Pi^{OPE}_{u} \not{u} + \Pi^{OPE}_{S} I + ... \tag{2.12}$$

Our main task in the following is to calculate the Π^{OPE}_{i} functions, where $i = \not{p}, \not{u}$ and I. Using the explicit forms of the interpolating currents in the correlation function in Eq. (2.1)

and contracting out all quark pairs via Wick's theorem, we find

$$
\begin{aligned}
\Pi_{\Sigma}^{OPE}(p) &= \frac{i}{2}\epsilon_{abc}\epsilon_{a'b'c'}\int d^4x e^{ipx}\Big\langle \psi_0\Big|\Big\{\Big(\gamma_5 S_d^{ca'}(x)S_s'^{bb'}(x)S_u^{ac'}(x)\gamma_5 \\
&+ \gamma_5 S_u^{cb'}(x)S_s'^{aa'}(x)S_d^{bc'}(x)\gamma_5 + \gamma_5 S_u^{cc'}(x)\gamma_5 Tr\Big[S_s^{ab'}(x)S_d'^{ba'}(x)\Big] \\
&+ \gamma_5 S_d^{cc'}(x)\gamma_5 Tr\Big[S_u^{ab'}(x)S_s'^{ba'}(x)\Big]\Big) + \beta\Big(\gamma_5 S_d^{ca'}(x)\gamma_5 S_s'^{bb'}(x)S_u^{ac'}(x) \\
&+ \gamma_5 S_u^{cb'}(x)\gamma_5 S_s'^{aa'}(x)S_d^{bc'}(x) + S_d^{ca'}(x)S_s'^{bb'}(x)\gamma_5 S_u^{ac'}(x)\gamma_5 \\
&+ S_u^{cb'}(x)S_s'^{aa'}(x)\gamma_5 S_d^{bc'}(x)\gamma_5 + \gamma_5 S_u^{cc'}(x)Tr\Big[S_s^{ab'}(x)\gamma_5 S_d'^{ba'}(x)\Big] \\
&+ S_u^{cc'}(x)\gamma_5 Tr\Big[S_s^{ab'}(x)S_d'^{ba'}(x)\gamma_5\Big] + \gamma_5 S_d^{cc'}(x)Tr\Big[S_u^{ab'}(x)\gamma_5 S_s'^{ba'}(x)\Big] \\
&+ S_d^{cc'}(x)\gamma_5 Tr\Big[S_u^{ab'}(x)S_s'^{ba'}(x)\gamma_5\Big]\Big) + \beta^2\Big(S_d^{ca'}(x)\gamma_5 S_s'^{bb'}(x)\gamma_5 S_u^{ac'}(x) \\
&+ S_u^{cb'}(x)\gamma_5 S_s'^{aa'}(x)\gamma_5 S_d^{bc'}(x) + S_u^{cc'}(x)Tr\Big[S_d^{ba'}(x)\gamma_5 S_s'^{ab'}(x)\gamma_5\Big] \\
&+ S_d^{cc'}(x)Tr\Big[S_s^{ba'}(x)\gamma_5 S_u'^{ab'}(x)\gamma_5\Big]\Big)\Big\}\Big|\psi_0\Big\rangle, \qquad (2.13)
\end{aligned}
$$

$$
\begin{aligned}
\Pi_{\Lambda}^{OPE}(p) &= -\frac{i}{6}\epsilon_{abc}\epsilon_{a'b'c'}\int d^4x e^{ipx}\Big\langle \psi_0\Big|\Big\{\Big(\gamma_5 S_d^{ca'}(x)S_s'^{bb'}(x)S_u^{ac'}(x)\gamma_5 \\
&+ 2\gamma_5 S_d^{ca'}(x)S_u'^{ab'}(x)S_s^{bc'}(x)\gamma_5 + 2\gamma_5 S_s^{ca'}(x)S_u'^{ab'}(x)S_d^{bc'}(x)\gamma_5 \\
&+ 2\gamma_5 S_s^{cb'}(x)S_d'^{ba'}(x)S_u^{ac'}(x)\gamma_5 + 2\gamma_5 S_u^{cb'}(x)S_d'^{ba'}(x)S_s^{ac'}(x)\gamma_5 \\
&+ \gamma_5 S_u^{cb'}(x)S_s'^{aa'}(x)S_d^{bc'}(x)\gamma_5 - \gamma_5 S_u^{cc'}(x)\gamma_5 Tr\Big[S_s^{ab'}(x)S_d'^{ba'}(x)\Big] \\
&- 4\gamma_5 S_s^{cc'}(x)\gamma_5 Tr\Big[S_u^{ab'}(x)S_d'^{ba'}(x)\Big] - \gamma_5 S_d^{cc'}(x)\gamma_5 Tr\Big[S_u^{ab'}(x)S_s'^{ba'}(x)\Big]\Big) \\
&+ \beta\Big(\gamma_5 S_d^{ca'}(x)\gamma_5 S_s'^{bb'}(x)S_u^{ac'}(x) + 2\gamma_5 S_d^{ca'}(x)\gamma_5 S_u'^{ab'}(x)S_s^{bc'}(x) \\
&+ 2\gamma_5 S_s^{ca'}(x)\gamma_5 S_u'^{ab'}(x)S_d^{bc'}(x) + 2\gamma_5 S_s^{cb'}(x)\gamma_5 S_d'^{ba'}(x)S_u^{ac'}(x) \\
&+ 2\gamma_5 S_u^{cb'}(x)\gamma_5 S_d'^{ba'}(x)S_s^{ac'}(x) + \gamma_5 S_u^{cb'}(x)\gamma_5 S_s'^{aa'}(x)S_d^{bc'}(x) \\
&+ S_d^{ca'}(x)S_s'^{bb'}(x)\gamma_5 S_u^{ac'}(x)\gamma_5 + 2S_d^{ca'}(x)S_u'^{ab'}(x)\gamma_5 S_s^{bc'}(x)\gamma_5 \\
&+ 2S_s^{ca'}(x)S_u'^{ab'}(x)\gamma_5 S_d^{bc'}(x)\gamma_5 + 2S_s^{cb'}(x)S_d'^{ba'}(x)\gamma_5 S_u^{ac'}(x)\gamma_5 \\
&+ 2S_u^{cb'}(x)S_d'^{ba'}(x)\gamma_5 S_s^{ac'}(x)\gamma_5 + S_u^{cb'}(x)S_s'^{aa'}(x)\gamma_5 S_d^{bc'}(x)\gamma_5 \\
&- \gamma_5 S_u^{cc'}(x)Tr\Big[S_s^{ab'}(x)\gamma_5 S_d'^{ba'}(x)\Big] - S_u^{cc'}(x)\gamma_5 Tr\Big[S_s^{ab'}(x)S_d'^{ba'}(x)\gamma_5\Big] \\
&- 4\gamma_5 S_s^{cc'}(x)Tr\Big[S_u^{ab'}(x)\gamma_5 S_d'^{ba'}(x)\Big] - \gamma_5 S_d^{cc'}(x)Tr\Big[S_u^{ab'}(x)\gamma_5 S_s'^{ba'}(x)\Big] \\
&- 4S_s^{cc'}(x)\gamma_5 Tr\Big[S_u^{ab'}(x)S_d'^{ba'}(x)\gamma_5\Big] - S_d^{cc'}(x)\gamma_5 Tr\Big[S_u^{ab'}(x)S_s'^{ba'}(x)\gamma_5\Big]\Big)
\end{aligned}
$$

$$
\begin{aligned}
&+ \beta^2\Big(S_d^{ca'}(x)\gamma_5 S_s'^{bb'}(x)\gamma_5 S_u^{ac'}(x) + 2S_d^{ca'}(x)\gamma_5 S_u'^{ab'}(x)\gamma_5 S_s^{bc'}(x)\\
&+ 2S_s^{ca'}(x)\gamma_5 S_u'^{ab'}(x)\gamma_5 S_d^{bc'}(x)\Big) + 2S_s^{cb'}(x)\gamma_5 S_d'^{ba'}(x)\gamma_5 S_u^{ac'}(x)\\
&+ 2S_u^{cb'}(x)\gamma_5 S_d'^{ba'}(x)\gamma_5 S_s^{ac'}(x) + S_u^{cb'}(x)\gamma_5 S_s'^{aa'}(x)\gamma_5 S_d^{bc'}(x)\\
&- S_u^{cc'}(x)Tr\Big[S_d^{ba'}(x)\gamma_5 S_s'^{ab'}(x)\gamma_5\Big] - 4S_s^{cc'}(x)Tr\Big[S_d^{ba'}(x)\gamma_5 S_u'^{ab'}(x)\gamma_5\Big]\\
&- S_d^{cc'}(x)Tr\Big[S_s^{ba'}(x)\gamma_5 S_u'^{ab'}(x)\gamma_5\Big]\Big\}\Big|\psi_0\Big\rangle, \qquad (2.14)
\end{aligned}
$$

$$
\begin{aligned}
\Pi_{\Xi}^{OPE}(p) &= i\epsilon_{abc}\epsilon_{a'b'c'}\int d^4x e^{ipx}\Big\langle\psi_0\Big|\Big\{\Big(-\gamma_5 S_s^{cb'}(x)S_u'^{ba'}(x)S_s^{ac'}(x)\gamma_5\\
&+ \gamma_5 S_s^{cc'}(x)\gamma_5 Tr\Big[S_s^{ab'}(x)S_u'^{ba'}(x)\Big]\Big) - \beta\Big(\gamma_5 S_s^{cb'}(x)\gamma_5 S_u'^{ba'}(x)S_s^{ac'}(x)\\
&+ S_s^{cb'}(x)S_u'^{ba'}(x)\gamma_5 S_s^{ac'}(x)\gamma_5 - \gamma_5 S_s^{cc'}(x)Tr\Big[S_s^{ab'}(x)\gamma_5 S_u'^{ba'}(x)\Big]\\
&- S_s^{cc'}(x)\gamma_5 Tr\Big[S_s^{ab'}(x)S_u'^{ba'}(x)\gamma_5\Big]\Big) + \beta^2\Big(-S_s^{cb'}(x)\gamma_5 S_u'^{ba'}(x)\gamma_5 S_s^{ac'}(x)\\
&+ S_s^{cc'}(x)Tr\Big[S_u^{ba'}(x)\gamma_5 S_s'^{ab'}(x)\gamma_5\Big]\Big)\Big\}\Big|\psi_0\Big\rangle, \qquad (2.15)
\end{aligned}
$$

where $S' = CS^TC$, $S_{u,d,s}$ are light quarks propagators and $Tr[...]$ denotes the trace of gamma matrices. In coordinate-space, the light quark propagator at the nuclear medium has the following form in the fixed-point gauge [18]:

$$
\begin{aligned}
S_q^{ab}(x) &\equiv \langle\psi_0|T[q^a(x)\bar{q}^b(0)]|\psi_0\rangle_{\rho_N}\\
&= \frac{i}{2\pi^2}\delta^{ab}\frac{1}{(x^2)^2}\not{x} - \frac{m_q}{4\pi^2}\delta^{ab}\frac{1}{x^2}\\
&+ \chi_q^a(x)\bar{\chi}_q^b(0) - \frac{ig_s}{32\pi^2}F_{\mu\nu}^A(0)t^{ab,A}\frac{1}{x^2}[\not{x}\sigma^{\mu\nu} + \sigma^{\mu\nu}\not{x}] + ..., \qquad (2.16)
\end{aligned}
$$

where ρ_N is the nuclear matter density, χ_q^a and $\bar{\chi}_q^b$ are the Grassmann background quark fields and $F_{\mu\nu}^A$ are classical background gluon fields (for details see [18]).

The invariant $\Pi_i^{OPE}(p)$ functions in the Borel scheme for each hyperon can be written in terms of the perturbative part and non-perturbative parts up to dimension six as following

$$
\widehat{\mathbf{B}}\Pi_i^{OPE}(p) = \widehat{\mathbf{B}}\Pi_i{}^{Pert} + \widehat{\mathbf{B}}\Pi_{i,D3}^{Non-pert} + \widehat{\mathbf{B}}\Pi_{i,D4}^{Non-pert} + \widehat{\mathbf{B}}\Pi_{i,D5}^{Non-pert} + \widehat{\mathbf{B}}\Pi_{i,D6}^{Non-pert}. \quad (2.17)
$$

The perturbative parts for all structures and the considered hyperons are found as

$$
\left.
\begin{aligned}
&\widehat{\mathbf{B}}\Pi_p^{Pert} = -\tfrac{1}{2048\pi^4}[5 + 2\beta + 5\beta^2]\int_0^{s_0} s^2 e^{-\frac{s}{M^2}}ds\\
&\widehat{\mathbf{B}}\Pi_u^{Pert} = 0\\
&\widehat{\mathbf{B}}\Pi_S^{Pert} = -\tfrac{1}{512\pi^4}(\beta-1)[3(\beta+1)(m_u+m_d) + (\beta-1)m_s]\int_0^{s_0} s^2 e^{-\frac{s}{M^2}}ds
\end{aligned}
\right\} \text{for } \Sigma, \qquad (2.18)
$$

$$\left.\begin{array}{l}\widehat{\mathbf{B}}\Pi_p^{Pert}=-\frac{1}{2048\pi^4}[5+\beta(2+5\beta)]\int_0^{s_0}s^2e^{-\frac{s}{M^2}}ds\\ \widehat{\mathbf{B}}\Pi_u^{Pert}=0\\ \widehat{\mathbf{B}}\Pi_S^{Pert}=-\frac{1}{1536\pi^4}(\beta-1)[(5\beta+1)(m_u+m_d)+(11\beta+13)m_s]\int_0^{s_0}s^2e^{-\frac{s}{M^2}}ds\end{array}\right\}\text{for }\Lambda, \tag{2.19}$$

$$\left.\begin{array}{l}\widehat{\mathbf{B}}\Pi_p^{Pert}=-\frac{1}{2048\pi^4}[5+\beta(2+5\beta)]\int_0^{s_0}s^2e^{-\frac{s}{M^2}}ds\\ \widehat{\mathbf{B}}\Pi_u^{Pert}=0\\ \widehat{\mathbf{B}}\Pi_S^{Pert}=-\frac{1}{512\pi^4}(\beta-1)[(\beta-1)m_u+6(\beta+1)m_s]\int_0^{s_0}s^2e^{-\frac{s}{M^2}}ds\end{array}\right\}\text{for }\Xi. \tag{2.20}$$

The functions $\widehat{\mathbf{B}}\Pi_{i,D3}^{Non-pert},\widehat{\mathbf{B}}\Pi_{i,D4}^{Non-pert},\widehat{\mathbf{B}}\Pi_{i,D5}^{Non-pert},\widehat{\mathbf{B}}\Pi_{i,D6}^{Non-pert}$ in non-perturbative parts have very lengthy expressions. So, we only present the function $\widehat{\mathbf{B}}\Pi_{i,D3}^{Non-pert}$ for the structure $\not{p}$ and Σ particle, as an example. It is obtained as

$$\begin{aligned}\widehat{\mathbf{B}}\Pi_{\Sigma,D3}^{Non-pert} &= \frac{\langle\bar{d}g_s\sigma Gd\rangle_{\rho_N}+\langle\bar{u}g_s\sigma Gu\rangle_{\rho_N}}{128\pi^2M^2}(1-\beta^2)m_s(3M^2-2p_0^2)+\frac{\langle d^\dagger iD_0iD_0d\rangle_{\rho_N}}{48\pi^2}\\
&\times\ p_0\Big[(3+2\beta+3\beta^2)M^2-2(1+\beta^2)p_0^2\Big]+\frac{\langle d^\dagger g_s\sigma Gd\rangle_{\rho_N}+\langle u^\dagger g_s\sigma Gu\rangle_{\rho_N}}{576\pi^2M^2}\\
&\times\ p_0(1+\beta^2)(2p_0^2-3M^2)+\frac{\langle s^\dagger g_s\sigma Gs\rangle_{\rho_N}}{576\pi^2M^2}p_0(3+2\beta+3\beta^2)(2p_0^2-3M^2)\\
&+\ \frac{\langle\bar{d}iD_0iD_0d\rangle_{\rho_N}+\langle\bar{u}iD_0iD_0u\rangle_{\rho_N}}{8\pi^2M^2}p_0^2m_s(1-\beta^2)\\
&-\ \frac{\langle s^\dagger iD_0iD_0s\rangle_{\rho_N}}{48\pi^2M^2}p_0\Big[M^2(1+\beta)^2+2p_0^2(3+2\beta+3\beta^2)\Big]\\
&+\ \frac{\langle u^\dagger iD_0iD_0u\rangle_{\rho_N}}{48\pi^2M^2}p_0\Big[M^2(3+2\beta+3\beta^2)-2p_0^2(1+\beta^2)\Big]\\
&-\ \frac{i\langle d^\dagger iD_0d\rangle_{\rho_N}+i\langle u^\dagger iD_0u\rangle_{\rho_N}}{288\pi^2}\Big[8p_0^2(1+\beta^2)-(11+6\beta+11\beta^2)\int_0^{s_0}e^{-\frac{s}{M^2}}ds\Big]\\
&-\ \frac{i\langle s^\dagger iD_0s\rangle_{\rho_N}}{288\pi^2}\Big[8p_0^2(3+2\beta+3\beta^2)-(3-2\beta+3\beta^2)\int_0^{s_0}e^{-\frac{s}{M^2}}ds\Big]\\
&+\ 3\frac{\langle\bar{d}d\rangle_{\rho_N}+\langle\bar{u}u\rangle_{\rho_N}}{64\pi^2}m_s(-1+\beta^2)\int_0^{s_0}e^{-\frac{s}{M^2}}ds\\
&+\ \frac{\langle d^\dagger d\rangle_{\rho_N}+\langle u^\dagger u\rangle_{\rho_N}}{96\pi^2}p_0(1+\beta^2)\int_0^{s_0}e^{-\frac{s}{M^2}}ds\\
&+\ \frac{\langle s^\dagger s\rangle_{\rho_N}}{96\pi^2}p_0(3+2\beta+3\beta^2)\int_0^{s_0}e^{-\frac{s}{M^2}}ds,\end{aligned} \tag{2.21}$$

where s_0 is the continuum threshold and we ignored to present the terms containing the up and down quark masses. Equating the hadronic and OPE sides of the correlation functions,

we get

$$\begin{aligned}
\lambda_{H^+}^{*2} e^{-\mu_{H^+}^2/M^2} + \lambda_{H^-}^{*2} e^{-\mu_{H^-}^2/M^2} &= \Pi_p^{OPE}, \\
-\lambda_{H^+}^{*2} \Sigma_{\nu H^+} e^{-\mu_{H^+}^2/M^2} - \lambda_{H^-}^{*2} \Sigma_{\nu H^-} e^{-\mu_{H^-}^2/M^2} &= \Pi_u^{OPE}, \\
\lambda_{H^+}^{*2} m_{H^+}^* e^{-\mu_{H^+}^2/M^2} - \lambda_{H^-}^{*2} m_{H^-}^* e^{-\mu_{H^-}^2/M^2} &= \Pi_S^{OPE}. \qquad (2.22)
\end{aligned}$$

To find the eight unknowns $\lambda_{H^+}^*, \lambda_{H^-}^*, m_{H^+}^*, m_{H^-}^*, \Sigma_{\nu H^+}, \Sigma_{\nu H^-}, \mu_{H^+}$ and μ_{H^-}, we need five more equations which are found by applying derivatives with respect to $(-1/M^2)$ to both sides of Eq. (2.22). As a result, we get

$$\begin{aligned}
\lambda_{H^+}^{*2} \mu_{H^+}^2 e^{-\mu_{H^+}^2/M^2} + \lambda_{H^-}^{*2} \mu_{H^-}^2 e^{-\mu_{H^-}^2/M^2} &= \frac{d\Pi_p^{OPE}}{d(-1/M^2)}, \\
-\lambda_{H^+}^{*2} \Sigma_{\nu H^+} \mu_{H^+}^2 e^{-\mu_{H^+}^2/M^2} - \lambda_{H^-}^{*2} \Sigma_{\nu H^-} \mu_{H^-}^2 e^{-\mu_{H^-}^2/M^2} &= \frac{d\Pi_u^{OPE}}{d(-1/M^2)}, \\
\lambda_{H^+}^{*2} m_{H^+}^* \mu_{H^+}^2 e^{-\mu_{H^+}^2/M^2} - \lambda_{H^-}^{*2} m_{H^-}^* \mu_{H^-}^2 e^{-\mu_{H^-}^2/M^2} &= \frac{d\Pi_S^{OPE}}{d(-1/M^2)}, \\
\lambda_{H^+}^{*2} (\mu_{H^+}^2)^2 e^{-\mu_{H^+}^2/M^2} + \lambda_{H^-}^{*2} (\mu_{H^-}^2)^2 e^{-\mu_{H^-}^2/M^2} &= \frac{d^2\Pi_p^{OPE}}{d(-1/M^2)^2}, \\
-\lambda_{H^+}^{*2} \Sigma_{\nu H^+} (\mu_{H^+}^2)^2 e^{-\mu_{H^+}^2/M^2} - \lambda_{H^-}^{*2} \Sigma_{\nu H^-} (\mu_{H^-}^2)^2 e^{-\mu_{H^-}^2/M^2} &= \frac{d^2\Pi_u^{OPE}}{d(-1/M^2)^2}. \qquad (2.23)
\end{aligned}$$

By solving the above eight equations simultaneously, we get the following in-medium sum rules for the parameters under consideration

$$\begin{aligned}
\lambda_{H^+}^{*2} &= \left[\frac{-2Q_2^2Q_3 + 2Q_1Q_2Q_4 + Q_1Q_3Q_7 - Q_1^2Q_8 + Q_1\tilde{Q}}{2\tilde{Q}}\right] e^{\mu_{H^+}^2/M^2}, \\
\lambda_{H^-}^{*2} &= \left[\frac{-2Q_2^2Q_3 + 2Q_1Q_2Q_4 + Q_1Q_3Q_7 - Q_1^2Q_8 + Q_1\tilde{Q}}{2\tilde{Q}}\right] e^{\mu_{H^-}^2/M^2}, \\
m_{H^+}^* &= \left[\frac{2Q_2Q_3Q_6 - 2Q_1Q_4Q_6 - Q_3Q_5Q_7 + Q_1Q_5Q_8 - Q_5\tilde{Q}}{2Q_2^2Q_3 - 2Q_1Q_2Q_4 - Q_1Q_3Q_7 + Q_1^2Q_8 - Q_1\tilde{Q}}\right], \\
m_{H^-}^* &= \left[\frac{-2Q_2Q_3Q_6 + 2Q_1Q_4Q_6 + Q_3Q_5Q_7 - Q_1Q_5Q_8 + Q_5\tilde{Q}}{2Q_2^2Q_3 - 2Q_1Q_2Q_4 - Q_1Q_3Q_7 + Q_1^2Q_8 - Q_1\tilde{Q}}\right], \\
\Sigma_{\nu H^\pm} &= \left[\frac{-2Q_2Q_4 + Q_3Q_7 + Q_1Q_8 + \tilde{Q}}{2(Q_2^2 - Q_1Q_7)}\right], \\
\mu_{H^+}^{*2} &= \left[\frac{Q_1Q_8 - Q_3Q_7 + \tilde{Q}}{2(Q_1Q_4 - Q_2Q_3)}\right], \\
\mu_{H^-}^{*2} &= \left[\frac{Q_3Q_7 - Q_1Q_8 + \tilde{Q}}{2(Q_2Q_3 - Q_1Q_4)}\right], \qquad (2.24)
\end{aligned}$$

where

$$Q_1 = \Pi_p^{OPE}, Q_2 = \frac{d\Pi_p^{OPE}}{d(-1/M^2)},$$
$$Q_3 = \Pi_u^{OPE}, Q_4 = \frac{d\Pi_u^{OPE}}{d(-1/M^2)},$$
$$Q_5 = \Pi_S^{OPE}, Q_6 = \frac{d\Pi_S^{OPE}}{d(-1/M^2)},$$
$$Q_7 = \frac{d^2\Pi_p^{OPE}}{d(-1/M^2)^2}, Q_8 = \frac{d^2\Pi_u^{OPE}}{d(-1/M^2)^2}, \tag{2.25}$$

and $\tilde{Q} = \sqrt{(Q_3Q_7 - Q_1Q_8)^2 + 4(Q_2Q_3 - Q_1Q_4)(Q_2Q_8 - Q_4Q_7)}$. Here we shall remark that we choose the above roots for $\mu_{H^\pm}^{*2}$ among four roots obtained from the calculations.

3 Numerical results and discussion

In this section, we numerically analyze the QCD sum rules for the residues, masses and self energies of Σ, Λ and Ξ hyperons for both parities in nuclear matter. For this aim, the numerical values of the quark masses as well as the in-medium quark-quark, quark-gluon, gluon-gluon condensates are necessary inputs. Their numerical values are listed in table 1. Besides, we need to find the working regions of three auxiliary parameters, namely continuum threshold s_0, Borel mass parameter M^2 and the arbitrary mixing parameter β. The standard criteria for finding the reliable working regions for these helping parameters is that, the physical quantities show good stability with respect to these parameters in those regions.

The continuum threshold s_0 corresponds to the beginning of the continuum in the considered channels. $\sqrt{s_0} - m_H$ is the energy that we need to excite the particle to its first excited state with the same quantum numbers. We take this value in the interval $[0.3 - 0.5]$ GeV. In this interval, the numerical results show weak dependency on the continuum threshold. To determine the working region for the Borel mass parameter M^2, we take into account two criteria: suppression of the contributions of the higher states and the continuum compared to the pole contribution and the exceeding of the perturbative part to the non-perturbative contributions. More precisely, the upper bound on the Borel parameter is found by demanding that

$$\frac{\int_0^{s_0} ds\rho_{p,u,S}(s)e^{-s/M^2}}{\int_0^{\infty} ds\rho_{p,u,S}(s)e^{-s/M^2}} > 1/2, \tag{3.26}$$

where $\rho_{p,u,S}(s)$ are the spectral densities corresponding to different structures in the channels under consideration. The lower bound on this parameter is obtained requiring that the perturbative contribution is more than the non-perturbative one and the term with highest dimension contributes less than 10% to the whole OPE, i.e. the series of sum rules converge. Note that to find the Borel window we consider all the sum rules in Eqs. (2.22) and (2.23) and choose the one with relatively worst OPE convergence. Our numerical calculations show that the last sum rule in Eq. (2.23) has relatively worst OPE convergence but still satisfies the aforesaid criteria. We consider this sum rule and the above mentioned conditions to determine the "Borel Window" at different channels.

In the case of the mixing parameter β, we try to find a β for each channel with a large residue/continuum ratio, showing that the relative contribution of the ground state pole to the sum rules is largest. Considering these criteria and using all input parameters, in the following, we perform our numerical analyses for the hyperons under consideration.

3.1 Σ hyperon

The aforementioned criteria for determination of the working region for the Borel mass parameter lead to the region 1.3 GeV$^2 \leqslant M^2 \leqslant$ 1.9 GeV^2 for the Σ hyperon. From the previously said considerations for the fixing of the mixing parameter β, we find that for $cos\theta = -0.76$, where $\theta = tan^{-1}(\beta)$, the relative contribution of the ground state pole residue is largest for the Σ hyperon. Using these values, we plot the dependence of the residues, masses and vector self-energies of the positive and negative parity Σ particle on the Borel mass parameter in figures 1-3. These figures demonstrate good stabilities with respect to M^2 and show weak dependence on the continuum threshold s_0 at their working regions. Obtained from the figures 1-3, the average values of the residues, masses and vector self-energies of the positive and negative parity Σ hyperons are depicted in table 2. Taking $\rho_N \to 0$ in the OPE side, we can also calculate the numerical values of the residues and masses in vacuum. The ratios of the residues and masses in nuclear matter to those of the vacuum together with the ratios of the self-energies to the vacuum masses are listed in table 3. In this table, we also present the predictions existing in the literature for the positive parity baryon. A quick glance in this table shows that, there are considerable shifts in the parameters under consideration in nuclear matter compared to their vacuum values for both parities in Σ channel. The shift on the residue of positive parity is negative but it is positive for the negative parity state. The shifts are negative for the masses of both parities. The obtained result for the ratio of the masses for the positive parity state in the present work

Input parameters	Values
p_0	m_H
m_u ; m_d ; m_s	$2.3^{0.7}_{-0.5}\ MeV$; $4.83^{0.5}_{-0.3}\ MeV$; $95 \pm 5\ MeV$ [19]
$m_{\Sigma^+}; m_{\Sigma^-}$	$1192.642 \pm 0.024\ MeV$; $\approx 1620\ MeV$ [19]
$m_{\Lambda^+}; m_{\Lambda^-}$	$1115.683 \pm 0.006\ MeV$; $1405.13^{1.3}_{-1.0}\ MeV$ [19]
$m_{\Xi^+}; m_{\Xi^-}$	$1314.86 \pm 0.2\ MeV$[19] ; $1.8\ GeV$ [20]
ρ_N	$(0.11)^3\ GeV^3$ [18, 21, 22]
$\langle q^\dagger q\rangle_{\rho_N}$; $\langle s^\dagger s\rangle_{\rho_N}$	$\frac{3}{2}\rho_N$; 0 [18, 21–23]
$\langle \bar{q}q\rangle_0$; $\langle \bar{s}s\rangle_0$	$(-0.241)^3\ GeV^3$; $0.8\ \langle \bar{q}q\rangle_0$ [24]
m_q	$0.5(m_u + m_d)$ [18, 21, 22]
σ_N ; σ_{N_0}	0.045 GeV ; 0.035 GeV [18, 21, 22]
y	0.04 ± 0.02 [25]; $0.066 \pm 0.011 \pm 0.002$ [26]
$\langle \bar{q}q\rangle_{\rho_N}$; $\langle \bar{s}s\rangle_{\rho_N}$	$\langle \bar{q}q\rangle_0 + \frac{\sigma_N}{2m_q}\rho_N$; $\langle \bar{s}s\rangle_0 + y\frac{\sigma_N}{2m_q}\rho_N$ [18, 21–23, 27]
$\langle q^\dagger g_s\sigma Gq\rangle_{\rho_N}$; $\langle s^\dagger g_s\sigma Gs\rangle_{\rho_N}$	$-0.33\ GeV^2\rho_N$; $-y0.33\ GeV^2\rho_N$ [18, 21–23, 27]
$\langle q^\dagger iD_0q\rangle_{\rho_N}$; $\langle s^\dagger iD_0s\rangle_{\rho_N}$	$0.18\ GeV\rho_N$; $\frac{m_s\langle \bar{s}s\rangle_{\rho_N}}{4} + 0.02\ GeV\rho_N$ [18, 21–23, 27]
$\langle \bar{q}iD_0q\rangle_{\rho_N}$; $\langle \bar{s}iD_0s\rangle_{\rho_N}$	$\frac{3}{2}m_q\rho_N \simeq 0$; 0 [18, 21–23, 27]
m_0^2	$0.8\ GeV^2$ [24]
$\langle \bar{q}g_s\sigma Gq\rangle_0$; $\langle \bar{s}g_s\sigma Gs\rangle_0$	$m_0^2\langle \bar{q}q\rangle_0$; $m_0^2\langle \bar{s}s\rangle_0$
$\langle \bar{q}g_s\sigma Gq\rangle_{\rho_N}$;$\langle \bar{s}g_s\sigma Gs\rangle_{\rho_N}$	$\langle \bar{q}g_s\sigma Gq\rangle_0 + 3\ GeV^2\rho_N$; $\langle \bar{s}g_s\sigma Gs\rangle_0 + 3y\ GeV^2\rho_N$[18, 21–23, 27]
$\langle \bar{q}iD_0iD_0q\rangle_{\rho_N}$;$\langle \bar{s}iD_0iD_0s\rangle_{\rho_N}$	$0.3\ GeV^2\rho_N - \frac{1}{8}\langle \bar{q}g_s\sigma Gq\rangle_{\rho_N}$;
	$0.3y\ GeV^2\rho_N - \frac{1}{8}\langle \bar{s}g_s\sigma Gs\rangle_{\rho_N}$ [18, 21–23, 27]
$\langle q^\dagger iD_0iD_0q\rangle_{\rho_N}$;$\langle s^\dagger iD_0iD_0s\rangle_{\rho_N}$	$0.031\ GeV^2\rho_N - \frac{1}{12}\langle q^\dagger g_s\sigma Gq\rangle_{\rho_N}$;
	$0.031y\ GeV^2\rho_N - \frac{1}{12}\langle s^\dagger g_s\sigma Gs\rangle_{\rho_N}$ [18, 21–23, 27]
$\langle \frac{\alpha_s}{\pi}G^2\rangle_0$	$(0.33 \pm 0.04)^4\ GeV^4$ [24]
$\langle \frac{\alpha_s}{\pi}G^2\rangle_{\rho_N}$	$\langle \frac{\alpha_s}{\pi}G^2\rangle_0 - 0.65\ GeV\rho_N$ [18, 21, 22]

Table 1: Numerical values for input parameters. We use the average value $y = 0.05$ to perform the numerical analyses.

is close to those of [7, 18] within the errors. For the $\Sigma_{\nu\Sigma^+}/m_{\Sigma^+}$, our result shows a small difference with those of [7, 18]. This can be attributed to the different interpolating currents used in these works and the fact that, we take into accounts both the positive and negative parity baryons. When we compare the results of parameters of the positive and negative parity cases, we see that the absolute value of the shift in the residue of the negative parity is considerably more than that of the positive parity Σ. Meanwhile, the absolute value of

the shift on the mass for the negative parity is also higher than that of the positive parity. The ratio $\Sigma_{\nu\Sigma^+}/m_{\Sigma^+}$ is roughly 1.8 times more than the ratio $\Sigma_{\nu\Sigma^-}/m_{\Sigma^-}$. Using the relation $m^*_\Sigma = m_\Sigma + \Sigma^S_\Sigma$, we find the scalar self energy of the positive and the negative parity Σ to be -0.324 GeV and -0.748 GeV, respectively. Our results for remaining parameters may be checked by other phenomenological approaches as well as the future experiments.

$\lambda^*_{\Sigma^+}$ [GeV^3]	$\lambda^*_{\Sigma^-}$ [GeV^3]	$m^*_{\Sigma^+}$ [GeV]	$m^*_{\Sigma^-}$ [GeV]	$\Sigma_{\nu\Sigma^+}$ [GeV]	$\Sigma_{\nu\Sigma^-}$ [GeV]
0.013 ± 0.003	0.027 ± 0.006	0.924 ± 0.330	0.779 ± 0.287	0.350 ± 0.035	0.228 ± 0.023

Table 2: The numerical values of residues, masses and self energies of Σ hyperon with positive and negative parities.

	$\lambda^*_{\Sigma^+}/\lambda_{\Sigma^+}$	$\lambda^*_{\Sigma^-}/\lambda_{\Sigma^-}$	$m^*_{\Sigma^+}/m_{\Sigma^+}$	$m^*_{\Sigma^-}/m_{\Sigma^-}$	$\Sigma_{\nu\Sigma^+}/m_{\Sigma^+}$	$\Sigma_{\nu\Sigma^-}/m_{\Sigma^-}$
Present work	0.94 ± 0.22	1.47 ± 0.27	0.74 ± 0.14	0.51 ± 0.09	0.28 ± 0.06	0.15 ± 0.03
[7, 18]			0.78-0.85		0.18-0.19	

Table 3: The ration of parameters for Σ hyperon.

At the end of this part, we would like to compare our results for the positive parity Σ baryon with those of nucleon [5]. In the case of mass, the shift is negative for both the Σ baryon and nucleon, although the value of shift in the case of Σ is 5% less than the nucleon. As far as, the residue of the positive parity of the Σ hyperon is concerned, the shift is -6% while it is -10% for the nucleon [5].

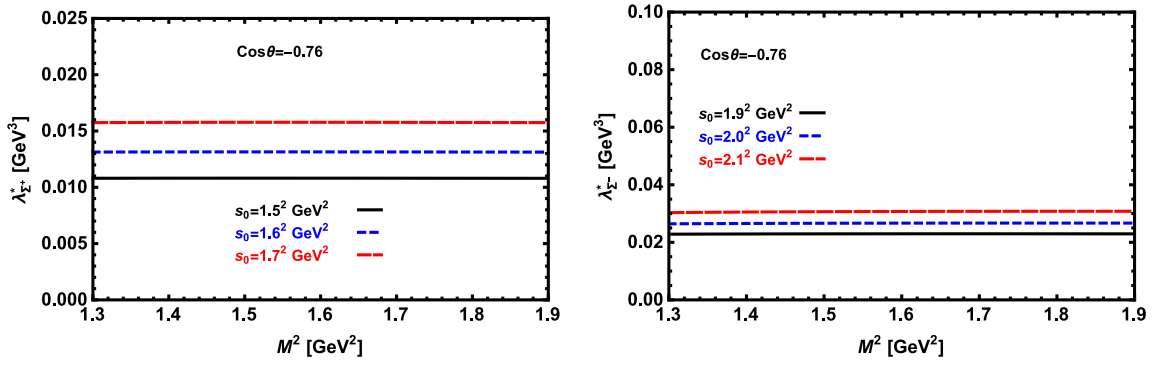

Figure 1: The residue of the positive parity Σ hyperon versus M^2 in nuclear matter (left panel). The same for negative parity Σ hyperon (right panel).

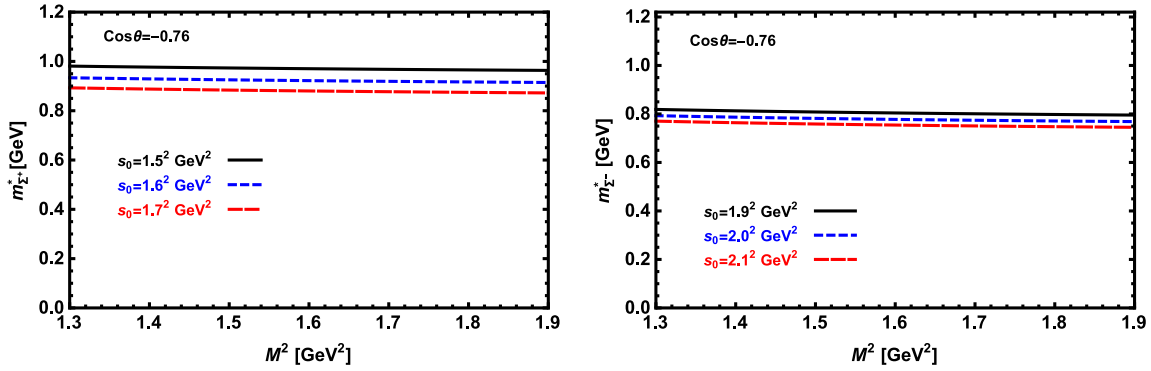

Figure 2: The mass of the positive parity Σ hyperon versus M^2 in nuclear matter (left panel). The same for negative parity Σ hyperon (right panel).

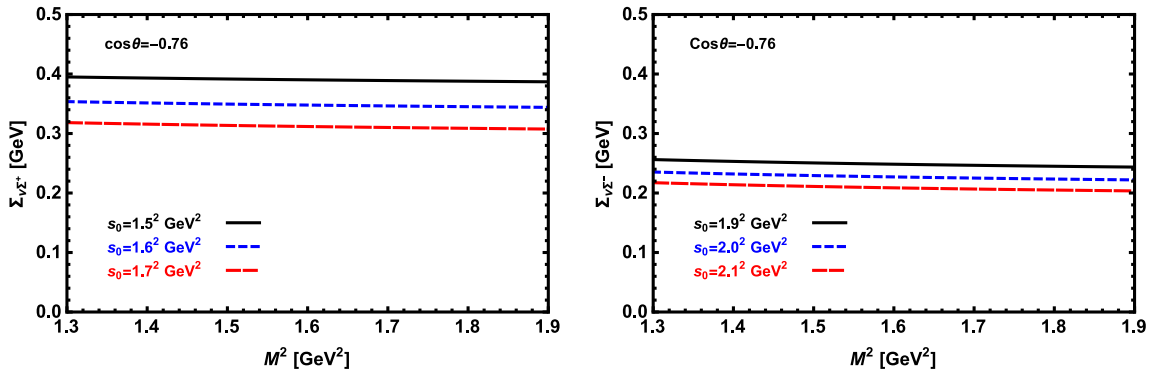

Figure 3: The self-energy of the positive parity Σ hyperon versus M^2 in nuclear matter (left panel). The same for negative parity Σ hyperon (right panel).

3.2 Λ hyperon

For the Λ hyperon, the interval of the Borel mass squared parameter is the same with Σ hyperon, i.e. $1.2\ GeV^2 \leqslant M^2 \leqslant 1.8\ GeV^2$. For this channel we find $cos\theta = -0.40$ demanding that the ratio residue/continuum is largest. By considering these values, we depict the dependence of the residues, masses and vector self-energies of the positive and negative parity Λ particle on the Borel mass parameter in figures 4-6. As expectedly, the behavior is similar to the Σ particle and we see good stabilities with respect to M^2 and the continuum threshold s_0 at their working regions. The numerical results gained from the figures 4-6 for the average values of the residues, masses and vector self-energies of the positive and negative Λ hyperon are presented in table 4. The ratios of the residues and masses in nuclear matter to those of the vacuum together with the ratios of the self-energies to the vacuum masses are listed in table 5. In this table, we also depict the predictions existing in the literature for the positive parity baryon. Similar to Σ channel results, this

table shows that there are considerable shifts in the parameters under consideration in nuclear matter compared to their vacuum values for both parities in Λ channel. The shift on the residues are positive while those are negative for the masses. The obtained result for the ratio of the masses for the positive parity baryon in the present work is close to that of [18] within the errors. In the comparison of the positive and negative parity parameters, the results show that the shifts in the residue and mass of the negative parity are considerably more than those of the positive parity Λ. When we compare the ratio $\Sigma_{\nu\Lambda^+}/m_{\Lambda^+}$ to the ratio $\Sigma_{\nu\Lambda^-}/m_{\Lambda^-}$, we find roughly 1.36 times differences. And finally, using the relation between the modified mass m^*_Λ and the vacuum mass m_Λ, we can easily find the scalar self energy of the positive and the negative parity Λ to be -0.102 GeV and -0.351 GeV, respectively. Our results for the remaining parameters can be verified by other phenomenological approaches as well as the future experiments.

$\lambda^*_{\Lambda^+}$ [GeV^3]	$\lambda^*_{\Lambda^-}$ [GeV^3]	$m^*_{\Lambda^+}$ [GeV]	$m^*_{\Lambda^-}$ [GeV]	$\Sigma^+_{\nu\Lambda}$ [GeV]	$\Sigma^-_{\nu\Lambda}$ [GeV]
0.024 ± 0.007	0.038 ± 0.008	1.022 ± 0.318	1.053 ± 0.158	0.193 ± 0.015	0.151 ± 0.052

Table 4: The numerical values of residues, masses and self energies of the Λ hyperon with positive and negative parities.

	$\lambda^*_{\Lambda^+}/\lambda_{\Lambda^+}$	$\lambda^*_{\Lambda^-}/\lambda_{\Lambda^-}$	$m^*_{\Lambda^+}/m_{\Lambda^+}$	$m^*_{\Lambda^-}/m_{\Lambda^-}$	$\Sigma_{\nu\Lambda^+}/m_{\Lambda^+}$	$\Sigma_{\nu\Lambda^-}/m_{\Lambda^-}$
Present work	1.87 ± 0.36	2.93 ± 0.53	0.91 ± 0.17	0.75 ± 0.13	0.17 ± 0.04	0.11 ± 0.02
[18]			0.85-0.94			

Table 5: The ratio of parameters for the Λ hyperon.

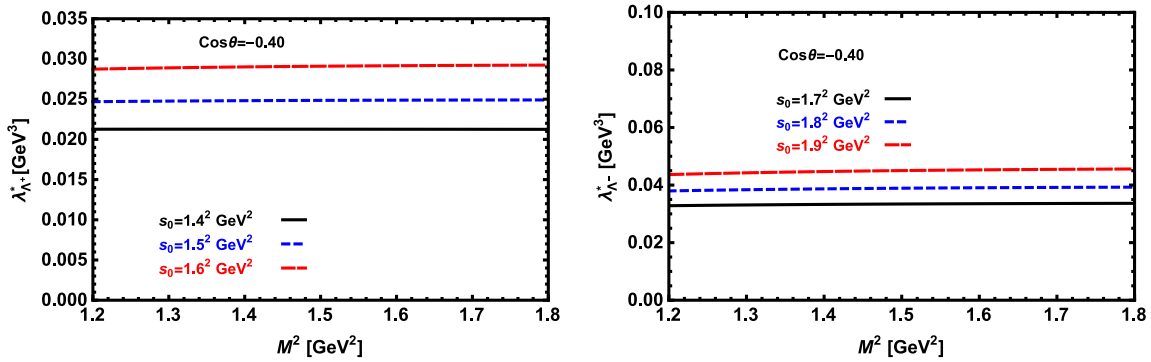

Figure 4: The residue of the positive parity Λ hyperon versus M^2 in nuclear matter (left panel). The same for negative parity Λ hyperon (right panel).

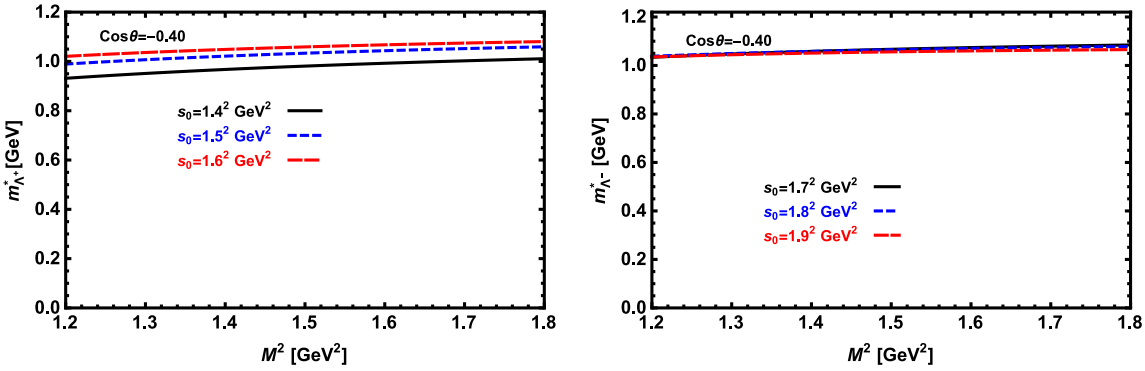

Figure 5: The mass of the positive parity Λ hyperon versus M^2 in nuclear matter (left panel). The same for negative parity Λ hyperon (right panel).

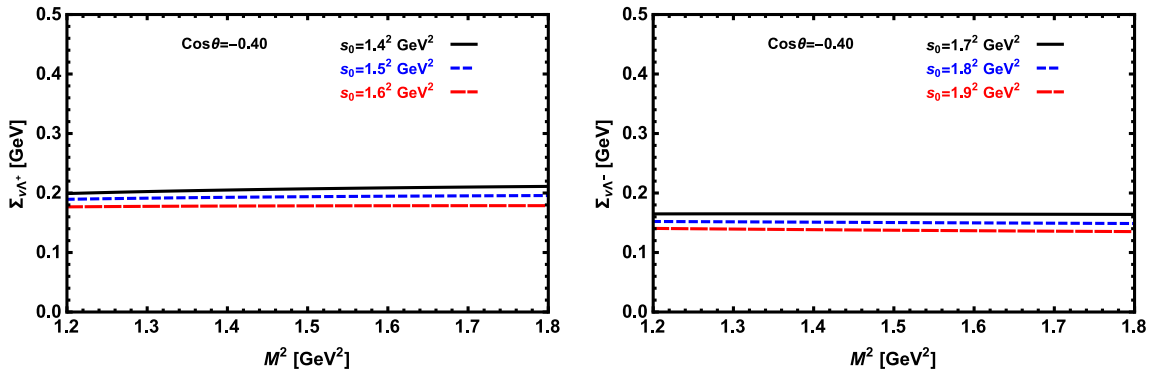

Figure 6: The self-energy of the positive parity Λ hyperon versus M^2 in nuclear matter (left panel). The same for negative parity Λ hyperon (right panel).

3.3 Ξ hyperon

In the Ξ hyperon channel, the interval 1.5 $GeV^2 \leqslant M^2 \leqslant$ 2.2 GeV^2 is chosen as the optimum region for the Borel mass squared parameter. We also find $cos\theta = -0.43$ for this channel in order to get highest residue/continuum ratio. We show the dependence of the residues, masses and vector self-energies of the positive and negative parity Ξ particle on the Borel mass parameter in figures 7-9. The numerical results acquired from these figures for the average values of the residues, masses and vector self-energies of the positive and negative parity Ξ hyperon are presented in table 6. The ratio of residues and masses in nuclear matter to those of the vacuum together with the ratio of self-energies to the vacuum masses are also demonstrated in table 7. With a quick look on this table, we obtained that there are also considerable shifts in the parameters under consideration in nuclear matter compared to their vacuum values for both parities in Ξ channel. The shift on the residues are again positive while those are negative for the masses. When we compare the results of

parameters of the positive and negative parity cases, we see that the shifts in the residue and mass of the negative parity are considerably more than those of the positive parity Ξ. With the help of the relation between m^*_Ξ and m_Ξ , it can be easily obtained that the scalar self energies of the positive and the negative parity Ξ are -0.116 GeV and -0.504 GeV, respectively. Our results on this channel also can be be tested via other approaches and experiments.

$\lambda^*_{\Xi+}$ [GeV^3]	$\lambda^*_{\Xi-}$ [GeV^3]	$m^*_{\Xi+}$ [GeV]	$m^*_{\Xi-}$ [GeV]	$\Sigma_{\nu\Xi+}$ [GeV]	$\Sigma_{\nu\Xi-}$ [GeV]
0.034 ± 0.009	0.065 ± 0.001	1.179 ± 0.351	1.124 ± 0.330	0.086 ± 0.026	0.044 ± 0.014

Table 6: The numerical values of the residues, masses and self energies of Ξ hyperon with positive and negative parities.

	$\lambda^*_{\Xi+}/\lambda_{\Xi+}$	$\lambda^*_{\Xi-}/\lambda_{\Xi-}$	$m^*_{\Xi+}/m_{\Xi+}$	$m^*_{\Xi-}/m_{\Xi-}$	$\Sigma_{\nu\Xi+}/m_{\Xi+}$	$\Sigma_{\nu\Xi-}/m_{\Xi-}$
Present work	2.05 ± 0.37	2.83 ± 0.49	0.91 ± 0.18	0.69 ± 0.12	0.07 ± 0.01	0.03 ± 0.00

Table 7: The ratio of parameters for the Ξ hyperon.

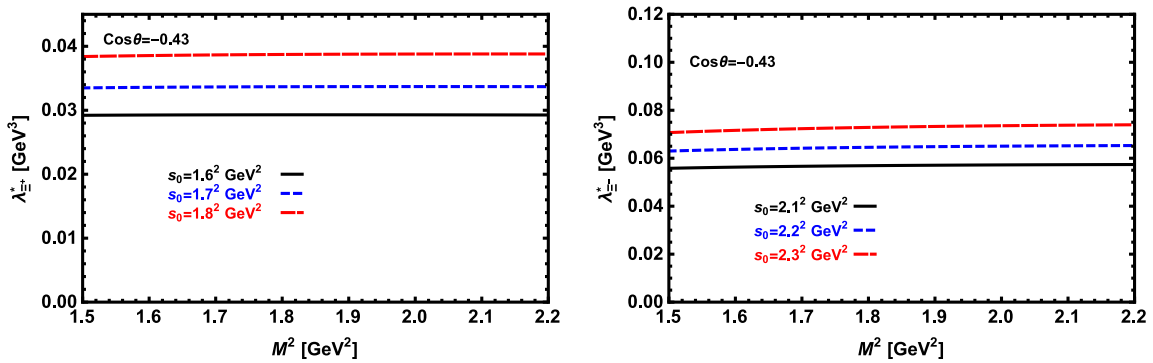

Figure 7: The residue of the positive parity Ξ hyperon versus M^2 in nuclear matter (left panel). The same for negative parity Ξ hyperon (right panel).

4 Concluding remarks

We investigated the effects of nuclear medium on the residues, masses and self-energies of the positive and negative parity Σ, Λ and Ξ hyperons in the framework of the QCD sum rule method. We used the general interpolating currents of these baryons with an arbitrary mixing parameter to calculate the shifts in the masses and residues of these

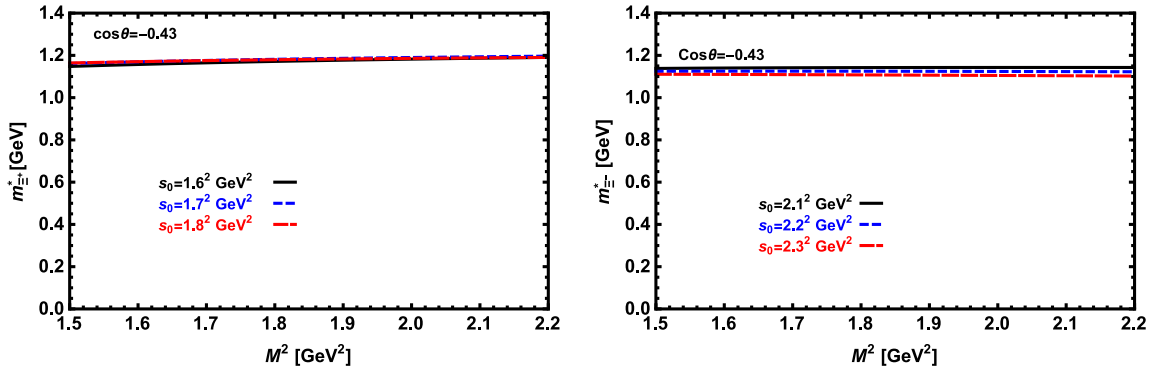

Figure 8: The mass of the positive parity Ξ hyperon versus M^2 in nuclear matter (left panel). The same for negative parity Ξ hyperon (right panel).

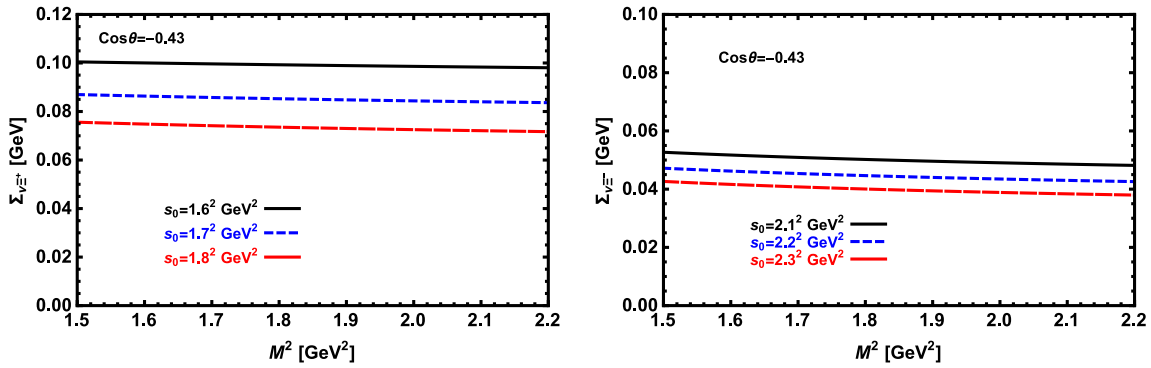

Figure 9: The self-energy of the positive parity Ξ hyperon versus M^2 in nuclear matter (left panel). The same for negative parity Ξ hyperon (right panel).

hyperons for both the positive and negative parity states in nuclear medium compared to their vacuum values. We also obtained the values of the vector and scalar self-energies for these baryons considering the reliable working regions of the auxiliary parameters entering the calculations. We observed that the shifts on the residues in nuclear matter are over all positive for both the positive and negative parity hyperons, except for the positive parity Σ hyperon that it is negative. The shifts on the masses of these baryons are obtained to be negative. It is found that the shifts on the residues and the masses corresponding to the negative parity particles are considerably large compared to those of the positive parity states. The maximum shift belong to the value of the residue of the negative parity Λ baryon. In the case of vector self-energy, the energy gained by the positive parity baryons are large in comparison with those of negative parity vector self-energy. The maximum value of the vector self-energy corresponds to the positive parity Σ hyperon. In the case of absolute value of the scalar self-energy, we found that the maximum and minimum values

belong to the negative parity Σ and the positive parity Λ hyperons, respectively. Our results can be checked via different phenomenological approaches as well as the future experiments. The obtained results can also be used in analyses of the heavy ion collision experiments.

5 Acknowledgement

This work has been supported in part by the Scientific and Technological Research Council of Turkey (TUBITAK) under the grant no: 114F018.

References

[1] E. G. Drukarev and E. M. Levin, Pis'ma Zh. Eksp. Teor. Fiz. 48, 307 (1988).

[2] E. G. Drukarev and E. M. Levin, Nucl. Phys. A 511, 679, (1990); 516, 715(E) (1990).

[3] T. Hatsuda, H. Hogaasen, M. Prakash, Phys. Rev. Lett. 66, 2851 (1991).

[4] C. Adami, G. E. Brown, Z. Phys. A 340, 93 (1991).

[5] K. Azizi, N. Er, Eur. Phys. J. C 74, 2904 (2014).

[6] Xuemin Jin and , R. J. Furnstahl, Phys. Rev. C 49, 1190 (1994).

[7] Xuemin Jin, Marina Nielsen, Phys. Rev. C51, 347 (1995).

[8] Martin J. Savage, Mark B. Wise, Phys.Rev. D53, 349-354 (1996).

[9] T. Miyatsu, K. Saito, Prog. Theor. Phys. 122, 1035-1044 (2009).

[10] S. R. Beane, E. Chang, S. D. Cohen, W. Detmold, H.-W. Lin, T. C. Luu, K. Orginos, A. Parreno, M. J. Savage, A. Walker-Loud, Phys. Rev. Lett. 109, 172001 (2012).

[11] V. Chung, H. G. Dosch, M. Kremer, D. Scholl, Nucl. Phys. B 197, 55 (1982).

[12] H. G. Dosch, M. Jamin and S. Narison, Phys. Lett. B 220, 251 (1989).

[13] R. Thomas, T. Hilger, B. Kampfer, Nucl. Phys. A 795, 19 (2007).

[14] E. G. Drukarev, M. G. Ryskin, V. A. Sadovnikova, arXiv:1312.1449[hep-ph].

[15] D. B. Leinweber, Phys. Rev. D 51, 6383 (1995).

[16] E. Stein, P. Gornicki, L. Mankiewicz, A. Schafer, W. Greiner, Phys. Lett. B 343, 369 (1995).

[17] T. D. Cohen, R. J. Furnstahl, and David K. Greigel, Phys. Rev. Lett. 67, 961 (1991).

[18] T. D. Cohen, R. J. Furnstahl, D. K. Griegel and Xuemin Jin, Prog. Part. Nucl. Phys. 35, 221 (1995).

[19] K.A. Olive et al. (Particle Data Group), Chin. Phys. C, 38, 090001 (2014).

[20] Yoshihiko Kondo, Osamu Morimatsu, Tetsuo Nishikawa, and Yoshiko Kanada-En'yo, Phys. Rev. D 75, 034010 (2007).

[21] T. D. Cohen, R. J. Furnstahl and D. K. Griegel, Phys. Rev. C 45, 1881 (1992).

[22] X. Jin, T. D. Cohen, R. J. Furnstahl, and D. K. Griegel, Phys. Rev. C 47, 2882 (1993).

[23] Zhi-Gang Wang, Eur. Phys. J. C72, 2099 (2012).

[24] V. M. Belyaev, B. L. Ioffe, Sov. Phys. JETP 57, 716 (1983); B. L. Ioffe,Prog. Part. Nucl. Phys. 56, 232 (2006).

[25] A. W. Thomas, P. E. Shanahan, R. D. Young, Nuovo Cim. C 035N04, 3 (2012).

[26] S. Dinter, V. Drach, K. Jansen, Int. J. Mod. Phys. Proc. Suppl. E 20, 110 (2011).

[27] X. Jin, M. Nielsen, T. D. Cohen, R. J. Furnstahl, D. K. Griegel, Phys. Rev. C 49, 464 (1994).